RESEARCH

Quantitative regional cerebral blood flow measurement using near-infrared spectroscopy and indocyanine green in patients undergoing superficial temporal to middle cerebral artery bypass for moyamoya disease: a novel method using a frequency filter

Akito Tsukinaga[1] · Kenji Yoshitani[1] · Takeo Ozaki[2] · Jun C. Takahashi[3] · Soshiro Ogata[4] · Yoshihiko Ohnishi[1]

Abstract

Measuring regional cerebral blood flow (rCBF) after revascularization for moyamoya disease, as a type of ischemic cerebrovascular disease, is crucial. This study aims to validate our novel technology that combines near-infrared spectroscopy (NIRS) with a frequency filter to extract the arterial component. We measured rCBF before and after revascularization for moyamoya disease and at the end of the surgery using NIRO-200NX (Hamamatsu Photonics, Japan) and indocyanine green (ICG). rCBF was calculated using Fick's principle, change in arterial ICG concentrations, and maximum arterial ICG concentration. rCBF measured with NIRS (rCBF_N) was compared with pre- and postoperative rCBF measured with SPECT (rCBF_S). Thirty-four procedures were analyzed. rCBF_N increased from baseline to end of the surgery (mean difference (MD), 2.99 ml/min/100 g; 95% confidence interval (CI), 0.40–5.57 ml/min/100 g on the diseased side; MD, 4.94 ml/min/100 g; 95% CI, 2.35–7.52 ml/min/100 g on the non-diseased side). Similar trends were observed for rCBF_S (MD, 3.98 ml/min/100 g; 95% CI, 2.30–5.67 ml/min/100 g on the diseased side; MD, 2.77 ml/min/100 g; 95% CI, 1.09–4.45 ml/min/100 g on the non-diseased side). Intraclass correlations 3 (ICC3s) between rCBF_N and rCBF_S were weak on the diseased side (ICC3, 0.25; 95% CI, -0.03–0.5; $p = 0.07$) and the non-diseased side (ICC3, 0.24; 95% CI, -0.05–0.5; $p = 0.08$). rCBF measurements based on this novel method were weakly correlated with rCBF measurements with SPECT.

Keywords Cerebrovascular circulation · Spectroscopy · Near-infrared · Indocyanine green · Moyamoya disease

---

✉ Kenji Yoshitani
ykenji@ncvc.go.jp

1   Department of Anesthesiology, National Cerebral and Cardiovascular Center, 6-1 Kishibeshimmachi, SuitaOsaka 564-8565, Japan

2   Systems Division, Hamamatsu Photonics K.K, Hamamatsu, Japan

3   Department of Neurosurgery, National Cerebral and Cardiovascular Center, Osaka, Japan

4   Department of Preventive Medicine and Epidemiology, National Cerebral and Cardiovascular Center, Osaka, Japan

1 Introduction

In patients with moyamoya disease, revascularization is recommended to prevent ischemic attacks by improving cerebral blood flow and reducing the risk of re-bleeding, especially in those at risk of intracerebral hemorrhage [1–3]. Several surgical procedures includes direct superficial temporal artery to middle cerebral artery (STA-MCA) bypass and indirect EDAS (encephalo-duro-arterio-synangiosis) procedure. Cerebral ischemia due to stenotic anastomosis is a devastating complication after STA-MCA bypass; the incidence is 4.7% [4]. To avoid postoperative cerebral ischemia due to STA graft stenosis, intraoperative direct flow Doppler has been used to measure flow velocity in the STA graft but it cannot quantify regional cerebral blood flow (rCBF). Postoperative transcranial Doppler provides bedside monitoring of blood velocity in large cerebral arteries. However, its accuracy is operator-dependent, and examiners cannot

find the signal in around 20% of patients. Velocity in the main arteries is an indirect measure of tissue perfusion [5]. Measuring rCBF after STA-MCA bypass is crucial because hypoperfusion or hyperperfusion might require additional treatment strategies.

Conventional methodologies for evaluating regional rCBF such as positron emission tomography (PET), single-photon emission tomography (SPECT), and perfusion computed tomography are implemented in radiologic facilities. Xenon computed tomography can be done at the bedside, but it is episodic and awkward to use. On the other hand, techniques combining near-infrared spectroscopy (NIRS) and indocyanine green (ICG) dye dilution to estimate cerebral hemodynamics have been developed [6–11]. In all studies, the optical density and arterial concentration of ICG have been quantified invasively either with an arterial fiberoptic catheter or high-performance liquid chromatography. Busch et al. and Milej et al. reported noninvasive optical monitoring of cerebral blood flow with diffuse correlation spectroscopy and contrast-enhanced NIRS, but the device is not commercially available [12, 13].

A noninvasive pulse dye–densitometer (Dye Densito-Gram Analyzer, Nihon Kohden Corp., Tokyo, Japan) enabled us to measure arterial ICG concentrations accurately via a finger or nasal probe. We were able to measure absolute rCBF (ml/min/100 g) easily at the bedside. However, the measurement of cerebral blood flow using the maximum slope method based on Fick's principle might not be accurate because of time resolution issues and contamination from venous blood [14].

NIRO-200NX (Hamamatsu Photonics K.K., Hamamatsu, Japan) is a commercially available cerebral oximeter with a sample rate of 20 Hz, which is ten times higher than a conventional NIRS oximeter. Based on the technology of the NIRO-200NX and a frequency filter to remove contamination from venous blood, we developed a quantitative method to measure rCBF. The purposes of the present study were to validate our novel technology involving NIRS and ICG for quantitative rCBF measurement and compare it to rCBF measured with quantitative SPECT in patients with moyamoya disease undergoing revascularization. We hypothesized that rCBF measured by NIRS at the end of surgery shows the same trend as rCBF measured by SPECT of 24 h difference in the measurements.

2 Methods

Consecutive patients undergoing elective STA-MCA bypass surgery for moyamoya disease were included in the study. The study was approved by the institutional ethics board on July 28, 2017 (study registration number, M29-027–2). The study was conducted from August 21, 2017 to March 31, 2022 in National Cerebral and Cardiovascular Center. Exclusion criteria included scalp wounds and iodine or ICG hypersensitivity. Study participants provided informed consent.

2.1 Anesthesia management

Anesthesia was maintained with sevoflurane and desflurane or propofol, fentanyl, and remifentanil. Patients were placed on mechanical ventilation with a tidal volume of 8–10 mL/kg body weight at a frequency of 8–12 breaths per minute to maintain $PaCO_2$ between 35 and 45 mmHg. Blood pressure was maintained around the patient's baseline with continuous phenylephrine infusion. Monitoring included electrocardiography, pulse oximetry, end-tidal carbon dioxide measurement, and invasive arterial blood pressure measurement.

2.2 Surgical procedure

In all patients, a single STA was anastomosed to the cortical MCA (M_4) in the frontal operculum with 11–0 nylon under a surgical microscope. The STA was harvested from the diseased side. No heparin was administered during the anastomosis.

2.3 Measurement of rCBF with NIRS

NIRO-200NX was used to measure rCBF based on the maximum slope method and Fick's principle. ICG has specific absorption properties for near-infrared light, which enables the measurement of changes in blood concentration of ICG with NIRO-ICG software (Hamamatsu Photonics K.K.) [15].

After induction of general anesthesia, NIRS probes were placed above the eyebrows on the scalp bilaterally. Light-impervious surgical drapes covered the NIRS probes to avoid light absorption signal contamination in extracerebral tissues. We measured rCBF simultaneously on the operative and nonoperative sides at the following three time points: before the anastomosis, just after the anastomosis, and at the end of the surgery. As a tracer, 7.5 mg of ICG was injected before the anastomosis, just after the anastomosis, and at the end of the surgery. After obtaining hemodynamic stability, we injected ICG (2.5 mg/mL) through a forearm vein. After the first injection, we confirmed with NIRO-ICG software that the ICG concentration measured by NIRS returned to baseline before the next injection of ICG. The kinetics of an intravenous bolus of ICG was monitored using NIRO-200NX, which emits light in the near-infrared region at three distinct wavelengths (735, 810, and 850 nm). The receiving probe collected the scattered light at a sample rate of 20 Hz. Absolute changes in the concentration of ICG were calculated based on near-infrared light attenuation according to the modified Beer-Lambert law. The maximum ICG concentration was measured with pulse dye-densitometry using

a DDG analyzer ™ (Nihon Kohden Corp.). We recorded rCBF, PaCO$_2$, hemoglobin concentration, and arterial blood pressure at each measurement time point.

2.4 Calculation of rCBF

Data on absorbance changes at the three wavelengths measured with NIRO-200NX were recalculated for oxygenated hemoglobin concentration, deoxygenated hemoglobin concentration, and ICG concentration based on the modified Beer-Lambert law using NIRO-ICG software. Typical ICG concentration changes based on NIRO-ICG software are shown in Fig. 1.

2.5 Changes in ICG concentration

2.5.1 Fick principle

ICG tracer was introduced into cerebral circulation from arterial blood into brain tissue through the capillaries. Some ICG is discharged into venous blood and some is deposited in brain tissue. According to Fick's principle, rCBF is calculated with the following equation:

$$\frac{dQ(t)}{dt} = rCBF(Pa(t) - Pv(t))$$

where $Q(t)$ is the concentration of ICG that has accumulated in the tissue, $Pa(t)$ is the ICG concentration in the cerebral artery, and $Pv(t)$ is the ICG concentration in a cerebral vein.

Integrating both sides of the equation yields the following:

where $Q(t)$ is the recalculated change in ICG concentration using the modified Beer-Lambert law.

$$Q(t) = rCBF(\int Pa(t)dt - \int Pv(t)dt)$$

$$rCBF(ml/min/100g) = \frac{Q(t)}{\int Pa(t)dt - \int Pv(t)dt}$$

Within a very short time, before ICG has reached the vein, $\int Pv(t)$ can be regarded as zero. $\int Pv(t)dt = 0$

The following equation is used to obtain rCBF:

$$CBF(ml/min/100g) = \frac{Q(t)}{\int Pa(t)dt}$$

The measured ICG concentration includes ICG concentrations in both arterial and venous blood. The curve of the change in ICG concentration over time has a pulsatile component derived from the artery (Fig. 1). The time course of ICG concentrations in the cerebral artery, Pa(t), is obtained from ICG data obtained with the digital filter process described next.

2.5.2 Digital filtering process

We designed a digital filter to extract pulsatile component of the pulse wave for 20-Hz sample measurements. This filter was designed to extract pulse waves with the heart rate in the 50–90 bpm range. The digital filter coefficients for heartbeat extraction with 20-Hz sampling were as follows: ki (i: − 8–8): k0 = 0.1964, k1 or − 1 = 0.1429, k2 or − 2 = 0.0804, k3 or − 3 = − 0.0179, k4 or − 4 = − 0.0804, k5 or − 5 = − 0.0893, k6 or − 6 = − 0.0804, k7 or − 7 = − 0.0357, and k8 or -8 = -0.0179 (Fig. 2).
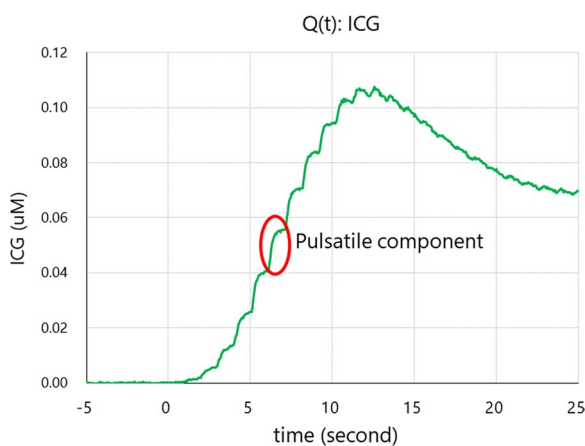

Fig. 1 ICG concentration changes measured with NIRO-ICG software. Typical waveform after injection of ICG (2.5 mg) into a forearm vein. The red circle indicates the pulsatile component of arterial origin. ICG, indocyanine green; Q(t), concentration of indocyanine green that has accumulated in the tissue
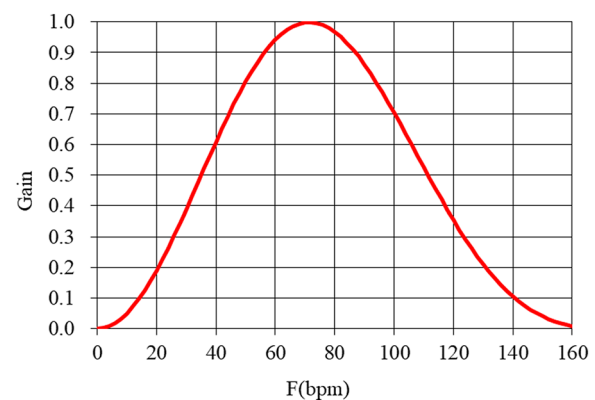

Fig. 2 Frequency response designed for the heartbeat (50–90 bpm). A digital filter was designed to extract the heart rate variability component. Digital filter coefficients are ki (i: − 8 to 8): k0 = 0.1964, k1 or − 1 = 0.1429, k2 or − 2 = 0.0804, k3 or − 3 = − 0.0179, k4 or − 4 = − 0.0804, k5 or − 5 = − 0.0893, k6 or − 6 = − 0.0804, k7 or − 7 = − 0.0357, and k8 or − 8 = − 0.0179

ICG(n) is the ICG signal sequence. ICG_p(n) is the ICG pulse wave signal sequence. ICG_p(n) is obtained from the following digital signal processing operation:

$$ICG_{\_p(n)} = \sum_{i=-8}^{+8} K_i * ICG(n+i)$$

ICG_p pulse wave signals after the processing described above are shown in Fig. 3A.

The amplitude of the ICG pulse wave changes rapidly. It reaches the maximum amplitude at approximately 7 s and decreases rapidly. The magnitude of the amplitude is thought to capture the change in ICG concentration in arterial blood. In other words, the function Amp(t), which reflects the change in amplitude, is considered to be proportional to the ICG concentration in arterial blood (Fig. 3B).

The amplitude value change function, Amp(t), traces the maximum value of each individual ICG_p pulse wave. The maximum ICG concentration in arterial blood from the simultaneous DDG analyzer measurement corresponds to the maximum value in this graph. From AMP(t), the ICG concentration function, Pa(t), in arterial blood can be quantified (Fig. 3C).

The denominator in Eq. (1) is the time-integrated function in Fig. 3C. Figure 3D shows the function obtained by substituting Q(t) in the numerator and ∫pa(t)dt into the denominator of the basic Eq. (1) for CBF. Although rCBF(t) is a function of time, the denominator is large, and the value of rCBF(t) is small after ICG reaches venous blood because the component of the ICG concentration that is discharged from venous blood is ignored. From the rCBF(t) function, the maximum value of rCBF(t) was calculated as rCBF because the maximum value of rCBF(t) is within the time-frame before ICG reaches venous blood.

2.6 Measurement of CBF with SPECT

To assess rCBF changes before and after surgery, quantitative N-isopropyl-p-[123I]-iodoamphetamine (123I-IMP) SPECT studies[16] were performed in patients using a triple-head gamma camera (GCA-9300R; Toshiba Medical Systems, Tokyo, Japan) at 2 days before surgery and on postoperative day 1 or 2. After intravenous infusion of 222 MBq of 123I-IMP, data acquisition was performed at a mean scan time of 30 min for 20 min. The CBF value of the upper anterior cerebral artery region corresponding to the NIRO-200NX probe attachment sites was used as the reference value. SPECT was suitable for measurement of rCBF in pediatric patients because of the difficulty adhering to face mask use for O^{15} gas inhalation during PET. In addition, SPECT was convenient to perform on the day after the surgery.
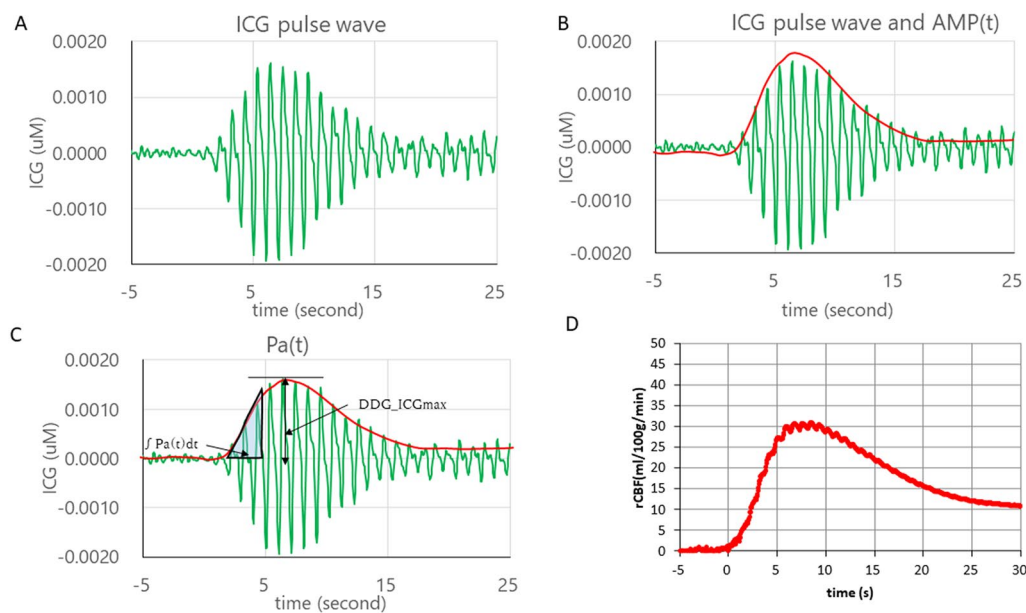

Fig. 3 **A** Pulse wave changes in ICG isolated from the curve of ICG concentration changes over time. **B** Pulse wave changes in ICG and Amp(t), the amplitude value change function. **C** Pulse wave changes in ICG, Amp(t), and Pa(t), the ICG concentration function in arterial blood calculated from Amp(t). D. The function obtained by substituting Q(t) into the numerator and ∫pa(t)dt into the denominator of the basic equation CBF = Q(t)/∫Pa(t) dt. Amp(t): amplitude value change function that traces the maximum value of each individual ICG pulse wave; DDG_ICGmax: maximum concentration of indocyanine green in arterial measured using the Dye DensitoGram Analyzer (Nihon Koden Corp., Tokyo, Japan); *ICG* indocyanine green; Pa(t): ICG concentration in the cerebral artery

2.7 Statistical analysis

Statistical analyses were performed using R version 4.05 (R Core Team, Vienna, Austria) and Stata version 17SE (College Station, TX, USA). For baseline patient characteristics, continuous variables are presented as means with standard deviations for normally distributed variables and were compared using the t-test. Non-normally distributed variables are presented as medians (interquartile range) and were compared using the Mann–Whitney U test. Categorical baseline variables were compared using Fisher's exact test. Repeated rCBF measurements with NIRO-200NX and SPECT were analyzed using a generalized linear mixed-effects model with random intercepts for each patient and diseased side and a random slope for measurement timing. Interactions between measurement timing and diseased side were also analyzed. Intraclass correlation coefficients (ICCs) case 3 between rCBF measured with NIRO-200NX and rCBF measured with SPECT were analyzed on the diseased and non-diseased sides to evaluate agreement in rCBF measurements between NIRO-200NX and SPECT. A p-value of < 0.05 for two-tailed tests and a p-value of < 0.1 for the interaction test were considered statistically significant. To evaluate agreement between rCBF measured with NIRO and rCBF measured with SPECT, we also performed Bland–Altman analysis.

3 Results

The study included 45 patients who underwent 51 procedures who met study eligibility criteria; 6 patients had STA-MCA bypass surgery on both sides. Due to missing rCBF values, 17 procedures were excluded from the analysis. The final analysis included 34 procedures in 31 patients, this includes three patients with bilateral procedure (Fig. 4). Missing data arose due to measurement equipment operation error or DDG analyzer ™ measurement error of ICG concentrations resulting from inadequate pulse pressure during the early phase of this study. Of the 31 patients, 19 were female. Mean (standard deviation) age, height, and body weight were 37.8 (16.5) years, 158.7 (12.6) cm, and 57.8 (15.8) kg, respectively. None of the patient developed postoperative ischemic events due to insufficient bypass flow. Maximum ICG concentration and hemoglobin gradually decreased. Heart rate, systolic blood pressure, and $PaCO_2$ remained constant during rCBF measurement (Supplementary Table 1).

Figure 5 shows the time course of changes in rCBF measured with NIRO-200NX and SPECT, respectively. The generalized linear mixed-effects model revealed that rCBF measured with NIRO-200NX increased from before anastomosis to the end of the surgery on both sides (mean
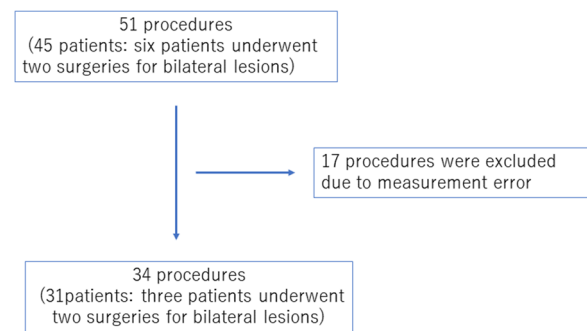

Fig. 4 Flow diagram. Procedure means superficial temporal artery to middle cerebral artery bypass surgery. Fifty-one procedures in 45 patients met the eligibility criteria and were enrolled. Due to missing rCBF values, 17 procedures were excluded from the analysis. Missing data arose due to measurement equipment operation error or DDG analyzer ™ measurement error resulting from inadequate pulse pressure

difference (MD), 2.99 ml/min/100 g; 95% confidence interval (CI), 0.40–5.57 ml/min/100 g; $p = 0.023$ on the diseased side; MD, 4.94 ml/min/100 g; 95% CI, 2.35–7.52 ml/min/100 g; $p < 0.001$ on the non-diseased side). rCBF measured with SPECT also increased from before surgery to after surgery on both sides (MD, 3.98 ml/min/100 g; 95% CI, 2.30–5.67 ml/min/100 g; $p < 0.001$ on the diseased side; MD, 2.77 ml/min/100 g; 95% CI, 1.09–4.45 ml/min/100 g; $p < 0.001$ on the non-diseased side).

There were no interactions between side and measurement time point in rCBF measured with NIRO-200NX ($p = 0.18$ just after anastomosis and 0.30 at the end of the surgery). There was an interaction for rCBF measured with SPECT ($p = 0.07$). There were no intraclass correlations between rCBF measured with SPECT and rCBF measured with NIRO-200NX (before anastomosis to just after anastomosis) on both sides (ICC3, 0.036; 95% CI; − 0.25–0.32; $p = 0.42$ on the diseased side; ICC3, 0.12; 95% CI, − 0.17–0.39; $p = 0.25$ on the non-diseased side). However, there were weak intraclass correlations between rCBF measured with SPECT and rCBF measured with NIRO-200NX (before anastomosis to end of the surgery) on the diseased and non-diseased sides (Table 1).

The agreement between cerebral blood flow measured by NIRO (CBF_N) and cerebral blood flow measured by SPECT (CBF_S) is shown in Fig. 6. Bland–Altman plots revealed that MD was − 1.1 ml/min/100 g and the limits of agreement were − 23.1 and 20.9 ml/min/100 g.

4 Discussion

The present study demonstrated weak intraclass correlations between rCBF measured with SPECT and rCBF measured with NIRO-200NX. Our novel methodology might be
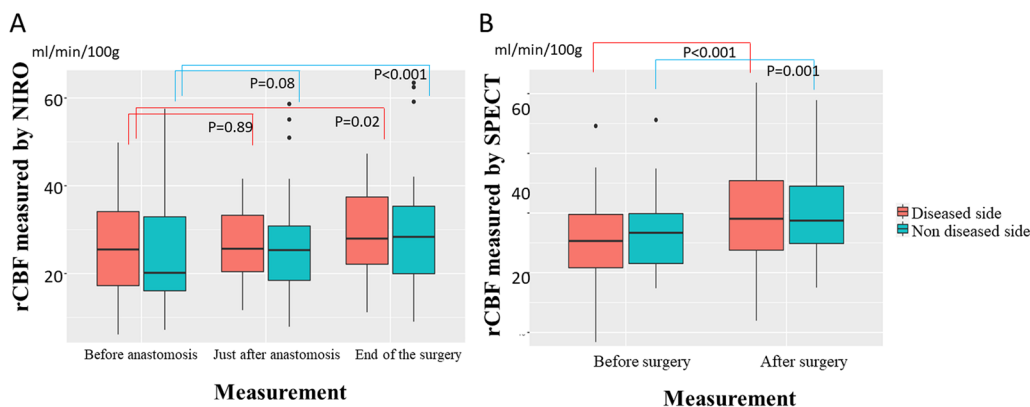
Fig. 5 A rCBF measured with NIRO-200NX. rCBF measured with NIRO-200NX increased from before anastomosis to the end of the surgery bilaterally. NIRO-200NX (Hamamatsu Photonics, Hamamatsu, Japan) is an oximeter that uses near-infrared spectroscopy. **B** rCBF measured with SPECT. rCBF measured with SPECT increased from before surgery to after surgery bilaterally, *rCBF* regional cerebral blood flow; *SPECT* single-photon emission computed tomography.

Table 1 Interclass correlation case3 between rCBF measured by NIRO and by Single photon emission tomography

	ICC3	P value (95% CI)
rCBF (before anastomosis to end of the surgery)		
Diseased side	0.25	0.070 (− 0.030 to 0.50)
Non diseased side	0.24	0.083 (-0.046 to 0.49)
rCBF (before anastomosis to just after anastomosis)		
Diseased side	0.036	0.42 (-0.20 to 0.28)
Non diseased side	0.12	0.25 (-0.17 to 0.39)

ICC3: Interclass correlation case3

clinically reliable for calculating rCBF. In addition, rCBF measured with NIRO-200NX increased after STA and MCA bypass, as did rCBF measured with SPECT.

There are several reasons why the intraclass correlation was weak between rCBF measured by NIRS and SPECT, the conventional CBF methodology. The timing of measurement after STA–MCA anastomosis was different for SPECT and NIRO-200NX: rCBF was measured at the end of the surgery with NIRO, but on postoperative day 1 or 2 with SPECT. Initially, quantitative cerebral blood flow measurement with SPECT included variations across among facilities and measurers [17]. After STA–MCA bypass, rCBF measured with SPECT and NIRO-200NX both showed an increasing trend. Therefore, a weak ICC was observed due to differences in the timing of measurements [18] and the small number of patients. rCBF measured with NIRO-200NX and SPECT increased postoperatively, which means that NIRO-200NX might be helpful for bedside rCBF measurement.

PET and SPECT are conventional methods for measuring CBF using radioisotopes as a tracer. However, PET and SPECT require patients to be transferred to a radiology facility. Therefore, rCBF was not measured in the operating room

or catheterization laboratory. On the other hand, measuring rCBF with NIRS and ICG as a tracer can be performed at the bedside in any location. Our goal is to establish a convenient rCBF measurement methodology.

Previous studies tried to measure rCBF using NIRS with ICG as a tracer. ICG is a known alternative to radioisotope tracers. ICG is used to measure cerebral blood volume [7]. Blood flow index based on the slope of change in ICG concentration measured with NIRS has been shown to be an indicator of the relative change in rCBF [11, 19, 20].

Other studies used Fick's principle to calculate rCBF, which requires maximum arterial ICG concentration and slope of the change in ICG concentration to measure CBF. ICG concentrations measured with NIRS reflect arterial and venous concentrations of ICG while ICG is certainly present in the large vessels. The extremely high absorption in these vessels produces a much lower NIRS signal and lower sensitivity to ICG concentrations within the vessels; it is difficult to distinguish the arterial component from the whole blood concentration every 0.05 s. As a result, previous studies measured arterial ICG concentrations using a dye densitometer unit (model DDG-2001A/K, Nihon Kohden Corp.) [14]. We developed a new methodology that distinguishes the arterial component from the whole blood concentration using a frequency filter. NIRO-200NX can measure changes in ICG concentration every 0.05 s, reflecting the waveform of the artery more accurately than NIRO-500. This short measurement interval is most advantageous for extracting the pulsatile arterial component. Yodh et al.[13] developed methods that can also differentiate waveforms. They have demonstrated that it is possible to quantitatively derive absolute CBF with ICG. However, the device is not commercially or clinically available. Furthermore, they used the ICG concentration change in the DDG analyzer ™ as the input function. Our method is more accurate because
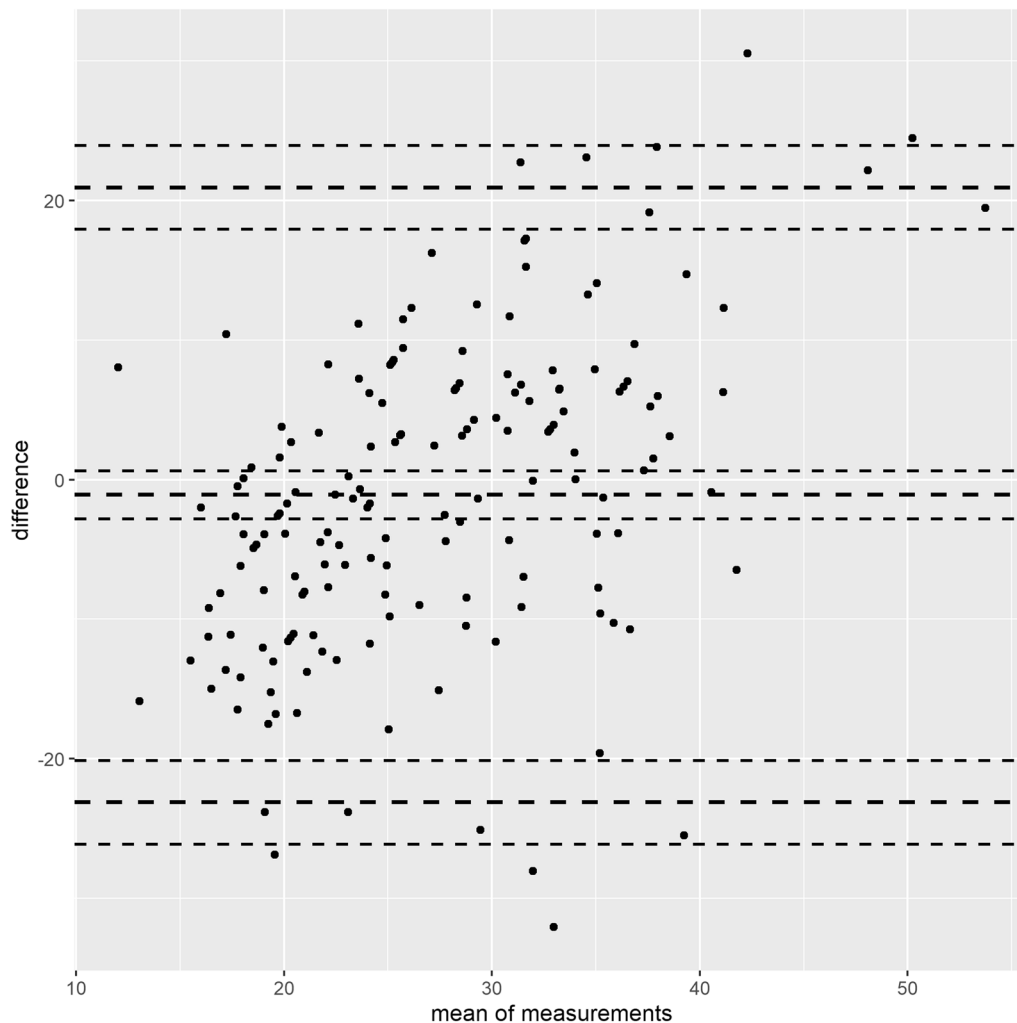
Fig. 6 Bland and Altman analysis between the cerebral blood flow measured by near infrared spectroscopy (NIRS) and by single photon emission tomography (SPECT). The limits of agreement represent the range within most differences between the 2 measurements will lie. Means of the measurements: means of regional cerebral blood flow (rCBF) measured by NIRS and SPECT. Difference: rCBF measured by NIRS – rCBF measured by SPECT

we separated the input function from the ICG concentration change in brain tissue.

According to the maximum slope method, rCBF is calculated based on the maximum slope of the curve and the maximum ICG concentration. The values obtained with this method are not considered to be very accurate because this method does not use the waveform in the denominator. Instead, it only uses the value at one time point, when ICG concentration peaks. On the other hand, our novel method obtains the input waveform for ICG using a frequency filter and applies a function to obtain changes in ICG concentration, instead of the maximum blood concentration of ICG used in the conventional maximum slope method. Thus, it can obtain more accurate rCBF values than the conventional maximum slope method. The arterial component could be separated using a frequency filter, although this was the

biggest challenge in measuring changes in ICG concentrations. This methodology is our unique method. We believe that this methodology that we developed has improved the accuracy of rCBF measurements. Venous saturation is calculated from NIRS pulse wave variability. Franceschini et al. and Lynch et al. focus on respiratory variability, which has a lower frequency than heart rate variability in previous studies [21, 22]. However, there have been no previous reports describing the use of a frequency filter as the input function for cerebral artery flow into brain tissue.

The present study has several limitations. First limitation: I addressed this already in methodology. rCBF might be affected by cardiac output, and the effect might be stronger in more impaired vessels. For rCBF measured with SPECT, there was a slight fluctuation in cardiac output because rCBF was measured while the patient was awake.

For rCBF measured with NIRO, hemodynamic status was stable during surgery, so the effect of fluctuations in cardiac output was considered negligible. Second, there were some missing data. However, bias due to missing data was minimal because a mixed-effects model was used. Measurement of rCBF with modified Lamber Beer law might include extracerebral contamination of approximately 10% of rSO_2 values [23], which might affect the measurement of rCBF. However, the advantages of rCBF measurement at the bedside using the commercially available NIRO 200NX device might overcome that limitation. Alternatives to modified Lamber Beer law should be considered in the future.

In conclusion, although it was not statistically significant, our novel method for measuring rCBF with NIRO-200NX was weakly correlated with rCBF measured with SPECT. This study indicates that rCBF could be measured at the bedside using ICG without going to radiology facilities in patients with severe disease. To validate rCBF measured with NIRS, further studies are required to compare rCBF values measured with NIRS and rCBF values measured with PET simultaneously.

Author contribution AT: This author was involved in data analysis, data interpretation, drafting of the manuscript and has approved the final version. KY: This author was involved in study design, data interpretation, drafting of the manuscript and has approved the final version. TO: This author was involved in data interpretation, commented on drafts of the manuscript, and has approved the final version. Moreover, the author developed the methodology of rCBF measurement using near-infrared spectroscopy. JCT: This author was involved in data interpretation, commented on drafts of the manuscript, and has approved the final version. SO: This author was involved in data analysis and data interpretation, commented on drafts of the manuscript, and has approved the final version. YO: This author was involved in study design, commented on drafts of the manuscript, and has approved the final version.

Declarations

Conflict of interest None of the authors have any conflicts of interest to declare. None of the authors have affiliations with Hamamatsu Photonics.

Ethical approval The study was approved by the institutional ethics board on July 28, 2017 (study registration number, M29-027–2).

Consent to participate Informed consent was obtained from all individual participants included in the study.

References

1. Tominaga T, Suzuki N, Miyamoto S, et al. Recommendations for the management of moyamoya disease: a statement from research committee on spontaneous occlusion of the circle of willis (Moyamoya Disease) [2nd Edition]. Surg Cereb Stroke. 2018;46(1):1–24. https://doi.org/10.2335/scs.46.1.
2. Miyamoto S, Yoshimoto T, Hashimoto N, et al. Effects of extracranial-intracranial bypass for patients with hemorrhagic moyamoya disease: results of the Japan Adult Moyamoya Trial. Stroke. 2014;45(5):1415–21. https://doi.org/10.1161/strokeaha.113.004386.
3. Takahashi JC, Funaki T, Houkin K, et al. Significance of the hemorrhagic site for recurrent bleeding: prespecified analysis in the japan adult moyamoya trial. Stroke. 2016;47(1):37–43. https://doi.org/10.1161/strokeaha.115.010819.
4. Kazumata K, Ito M, Tokairin K, et al. The frequency of postoperative stroke in moyamoya disease following combined revascularization: a single-university series and systematic review. J Neurosurg. 2014;121(2):432–40. https://doi.org/10.3171/2014.1.Jns13946.
5. He L, Wu DF, Zhang JH, Zheng S, Li Y, He W. Factors affecting transtemporal window quality in transcranial sonography. Brain Behav. 2022;12(4): e2543. https://doi.org/10.1002/brb3.2543.
6. Chow G, Roberts IG, Fallon P, et al. The relation between arterial oxygen tension and cerebral blood flow during cardiopulmonary bypass. Eur J Cardiothorac Surg. 1997;11(4):633–9. https://doi.org/10.1016/s1010-7940(96)01073-1.
7. Hopton P, Walsh TS. Lee A (1999) Measurement of cerebral blood volume using near-infrared spectroscopy and indocyanine green elimination. J Appl Physiol. 1985;87(5):1981–7. https://doi.org/10.1152/jappl.1999.87.5.1981.
8. Patel J, Marks K, Roberts I, Azzopardi D, Edwards AD. Measurement of cerebral blood flow in newborn infants using near infrared spectroscopy with indocyanine green. Pediatr Res. 1998;43(1):34–9. https://doi.org/10.1203/00006450-199801000-00006.
9. McCormick PW, Stewart M, Goetting MG, Dujovny M, Lewis G, Ausman JI. Noninvasive cerebral optical spectroscopy for monitoring cerebral oxygen delivery and hemodynamics. Crit Care Med. 1991;19(1):89–97. https://doi.org/10.1097/00003246-199101000-00020.
10. Roberts I, Fallon P, Kirkham FJ, et al. Estimation of cerebral blood flow with near infrared spectroscopy and indocyanine green. Lancet. 1993;342(8884):1425. https://doi.org/10.1016/0140-6736(93)92786-s.
11. Kuebler WM, Sckell A, Habler O, et al. Noninvasive measurement of regional cerebral blood flow by near-infrared spectroscopy and indocyanine green. J Cereb Blood Flow Metab. 1998;18(4):445–56. https://doi.org/10.1097/00004647-199804000-00013.
12. Busch DR, Balu R, Baker WB, et al. Detection of brain hypoxia based on noninvasive optical monitoring of cerebral blood flow with diffuse correlation spectroscopy. Neurocrit Care. 2019;30(1):72–80. https://doi.org/10.1007/s12028-018-0573-1.
13. Milej D, He L, Abdalmalak A, et al. Quantification of cerebral blood flow in adults by contrast-enhanced near-infrared spectroscopy: validation against MRI. J Cereb Blood Flow Metab. 2020;40(8):1672–84. https://doi.org/10.1177/0271678x19872564.
14. Gora F, Shinde S, Elwell CE, et al. Noninvasive measurement of cerebral blood flow in adults using near-infrared spectroscopy and indocyanine green: a pilot study. J Neurosurg Anesthesiol. 2002;14(3):218–22. https://doi.org/10.1097/00008506-200207000-00008.
15. Nakagawa I, Park HS, Yokoyama S, et al. Indocyanine green kinetics with near-infrared spectroscopy predicts cerebral hyperperfusion syndrome after carotid artery stenting. PLoS ONE.

2017;12(7): e0180684. https://doi.org/10.1371/journal.pone.0180684.

16. Mizumura S, Kumita S, Cho K, et al. Development of quantitative analysis method for stereotactic brain image: assessment of reduced accumulation in extent and severity using anatomical segmentation. Ann Nucl Med. 2003;17(4):289–95. https://doi.org/10.1007/bf02988523.

17. Iida H, Nakagawara J, Hayashida K, et al. Multicenter evaluation of a standardized protocol for rest and acetazolamide cerebral blood flow assessment using a quantitative SPECT reconstruction program and split-dose ^{123}I-Iodoamphetamine. J Nucl Med. 2010;51(10):1624–31. https://doi.org/10.2967/jnumed.110.078352.

18. Kameyama M, Fujimura M, Tashiro R, et al. significance of quantitative cerebral blood flow measurement in the acute stage after revascularization surgery for adult moyamoya disease: implication for the pathological threshold of local cerebral hyperperfusion. Cerebrovasc Dis. 2019;48(3–6):217–25. https://doi.org/10.1159/000504835.

19. Schytz HW, Wienecke T, Jensen LT, Selb J, Boas DA, Ashina M. Changes in cerebral blood flow after acetazolamide: an experimental study comparing near-infrared spectroscopy and SPECT. Eur J Neurol. 2009;16(4):461–7. https://doi.org/10.1111/j.1468-1331.2008.02398.x.

20. Kato S, Yoshitani K, Ohnishi Y. Cerebral blood flow measurement by near-infrared spectroscopy during carotid endarterectomy. J Neurosurg Anesthesiol. 2016;28(4):291–5. https://doi.org/10.1097/ana.0000000000000223.

21. Franceschini MA, Boas DA, Zourabian A, et al. (2002) Near-infrared spiroximetry: noninvasive measurements of venous saturation in piglets and human subjects. J Appl Physiol. 1985;92(1):372–84. https://doi.org/10.1152/jappl.2002.92.1.372.

22. Lynch JM, Buckley EM, Schwab PJ, et al. Noninvasive optical quantification of cerebral venous oxygen saturation in humans. Acad Radiol. 2014;21(2):162–7. https://doi.org/10.1016/j.acra.2013.10.013.

23. Sophie H. Impact of extracranial contamination on regional cerebral oxygen saturation. Anesthesiology. 2012;116(4):834–40. https://doi.org/10.1097/aln.0b013e31824c00d7.